2008 October 29

Trigonometric Parallaxes of Massive Star Forming Regions: II. Cep A & NGC 7538

L. Moscadelli[1], M. J. Reid[2], K. M. Menten[3], A. Brunthaler[3], X. W. Zheng[4] and Y. Xu[3,5]

ABSTRACT

We report trigonometric parallaxes for the sources NGC 7538 and Cep A, corresponding to distances of $2.65^{+0.12}_{-0.11}$ kpc and $0.70^{+0.04}_{-0.04}$ kpc, respectively. The distance to NGC 7538 is considerably smaller than its kinematic distance and places it in the Perseus spiral arm. The distance to Cep A is also smaller than its kinematic distance and places it in the "Local" arm or spur. Combining the distance and proper motions with observed radial velocities gives the location and full space motion of the star forming regions. We find significant deviations from circular Galactic orbits for these sources: both sources show large peculiar motions (> 10 km s^{-1}) counter to Galactic rotation and NGC 7538 has a comparable peculiar motion toward the Galactic center.

Subject headings: techniques: interferometric — masers — stars: distances — ISM: individual (NGC 7538, Cepheus A) — Galaxy: structure

1. Introduction

This paper is the second in a series of papers that describe the results of a large program to determine Galactic structure by measuring trigonometric parallaxes and proper motions. Trigonometric parallaxes provide the "gold standard" of distance measurements and can resolve fundamental questions of source luminosity, mass, and age.

---

[1]INAF, Osservatorio Astrofisico di Arcetri, Largo E. Fermi 5, 50125 Firenze, Italy

[2]Harvard-Smithsonian Center for Astrophysics, 60 Garden Street, Cambridge, MA 02138, USA

[3]Max-Planck-Institut für Radioastronomie, Auf dem Hügel 69, 53121 Bonn, Germany

[4]Department of Astronomy, Nanjing University Nanjing 210093, China

[5]Purple Mountain Observatory, Chinese Academy of Sciences, Nanjing 210008, China

The targets of our program are methanol (CH_3OH) masers associated with high-mass star forming regions. We used the National Radio Astronomy Observatory's [1] Very Long Baseline Array (VLBA) to conduct astrometic observations of the masers relative to compact extragalactic radio sources, and we have achieved parallax accuracies approaching ± 10 μas. Background information about our program is given in Reid et al. (2008), hereafter called Paper I.

In this paper we report VLBA observations of 12 GHz methanol masers toward NGC 7538 and Cep A. These well-studied sources are in the 2^{nd} quadrant of the Galaxy. NGC 7538 has a kinematic distance of about 5.6 kpc, which would place it well past the Perseus spiral arm, possibly in the "Outer" ("Cygnus") arm. However, Xu et al. (2006) found that the kinematic distance for W3OH, a source at a comparable Galactic longitude and kinematic distance, was a factor of two too great. So, obtaining a direct distance estimate is important to locate this source in the Galaxy. While Cep A is likely in the "Local" arm or spur, its distance is uncertain, with estimates ranging between 0.3 kpc (Migenes et al. 1992) and 0.9 kpc (Moreno-Corral et al. 1993). Here we present parallax measurements of NGC 7538 and Cep A.

2. Observations and Data Reduction

Paper I describes the general observational setup and method of calibration. Here we give only procedures and parameters specific to the observations of NGC 7538 and Cep A. We used the VLBA (program BR100C) to observe the $2_0 - 3_{-1}$ E (ν_0 = 12178.597 MHz) transition of methanol at five dates: 2005 September 9 and December 1 and 2006 February 25, May 26 and September 1. These dates were selected to symmetrically sample both the eastward and northward parallax signatures and minimize correlations among the parallax and proper motion parameters. The first, fourth and fifth observations were fully successful with a very low (<1%) level of observing downtime; for the second epoch the Brewster antenna did not produce fringes and for the third epoch Hancock did not observe due to bad weather.

In order to provide independent measures of parallax and reduce the risk of structural variability of the background source, we used two background continuum sources: J2254+6209 and J2302+6405. Table 1 lists the positions of the masers and the background sources. The dual circularly polarized 4 MHz bands containing the maser signals were cen-

[1] The National Radio Astronomy Observatory is a facility of the National Science Foundation operated under cooperative agreement by Associated Universities, Inc.

tered at LSR velocities ($V_{\rm LSR}$) of -10 km s^{-1} and -60 km s^{-1} for Cep A and NGC 7538, respectively. Spectral resolution was 0.38 km s^{-1}.

We used observations of the strong VLBA calibrator 3C 454.3 to correct for instrumental delays and phase offsets among different frequency bands. The spectral channel with the strongest maser emission was used as the phase reference: $V_{\rm LSR} = -4.2$ km s^{-1} for Cep A and $V_{\rm LSR} = -55.8$ km s^{-1} for NGC 7538. These reference features were detected at all epochs and were relatively stable, varying in intensity by less than $\pm 20\%$.

For the maser data, after phase referencing we produced naturally-weighted maps for each spectral channel, covering a region of $\approx 2''$. Our spectral resolution was inadequate to resolve some narrow maser features and, to minimize spectral sidelobes, we Hanning smoothed the visibilities, reducing the velocity resolution to ≈ 0.8 km s^{-1}. We searched all maser spectral channels for emission above a conservative threshold taken as the absolute value of the minimum in the map. This allows for dynamic range limitations, as opposed to using a strict map-noise limit. The detected maser spots were fitted with an elliptical Gaussians brightness distribution (using the AIPS task JMFIT).

The maser images for both sources were elongated and extended over a size of a few mas. This precluded using VLBA antennas that produced only long baselines that fully resolved the masers, since reference-phase solutions could not be obtained. Thus, compared to some other sources in our program, these observations had lower angular resolution. For both maser sources we used a circular restoring beam of 2 mas FWHM, which was close to the interferometer "dirty" beam.

The reference channel image for NGC 7538 revealed some asymmetric structure (see Fig. 1). Thus, we self-calibrated (amplitude and phase) the reference channel visibilities and applied the corrections to both the continuum and line data before mapping. This preserves the astrometric precision for relative position measurements. The Cep A reference channel was not strong enough to allow self-calibration. The image (see Fig. 4) shows symmetric low-level structures that are probably caused by small amplitude calibration errors. Since, for brightnesses $> 20\%$ of the peak, the source structure is relatively simple, resonable position accuracy could still be achieved.

For the background continuum sources (J2254+6209 and J2302+6405), we integrated the data from all four dual-polarized bands and imaged the sources using the AIPS task IMAGR. The naturally-weighted "dirty" beam was determined by the availability of maser phase-reference data and was almost circular with a FWHM of 1.9×1.8 mas. Matching the maser images, we adopted a circular restoring beam of 2 mas (FWHM).

Table 1. Positions and Brightnesses

Source	R.A. (J2000) (h m s)	Dec. (J2000) (° ' ")	ϕ (°)	P.A. (°)	Brightness (Jy/beam)	V_{LSR} (km s^{-1})
NGC 7538	23 13 45.3622	61 28 10.507			5–6	−57
J2254+6209	22 54 25.2930	62 09 38.725	2.4	−73	0.07	
J2302+6405	23 02 41.3150	64 05 52.849	2.9	−27	0.12	
Cep A	22 56 18.0970	62 01 49.399			0.6–1	−10
J2254+6209	22 54 25.2930	62 09 38.725	0.3	−59	0.07	
J2302+6405	23 02 41.3150	64 05 52.849	2.2	20	0.12	

Note. — ϕ and P.A. are the separations and position angles (East of North) from the maser to the reference sources. For both maser and quasar images, we used a circular restoring beam of 2 mas FWHM. For both maser targets, the derived absolute position of the reference maser channel is based on the position of the quasar J2302+6405 from the VLBA calibrator survey. The error in the absolute position of NGC 7538 is dominated by the uncertainty in the absolute position of the quasar J2302+6405, 0.26 mas and 0.48 mas in R.A. and Dec., respectively. For the weaker and extended Cep A maser (see discussion in Sect. 3.2), the R.A. position error is $\sim$1.3 mas.

3. Parallaxes and Proper Motions

We measured the parallax and proper motions of the 12 GHz masers from the change in the position differences of the masers with respect to the background continuum sources. The change in position of a maser spot relative to the background source was modeled as a combination of the parallax sinuisoid and a secular proper motion in each celestial coordinate. See Paper I for details of this procedure.

Since systematic errors, owing to maser blending, potential structure in the background continuum sources, and unmodeled atmospheric delay variations usually dominate over signal-to-noise limitations, we adopted an empirical approach to the weighting of the data. We added "error floors" in quadrature with the formal position uncertainties, separately to the east and north position offsets. These error floors were adjusted until the residuals of parallax and proper motion fit yielded a χ^2 per degree of freedom near unity in each coordinate.

3.1. NGC 7538

For NGC 7538, we found that spatial blending of maser features limited the accuracy of spot positions. We attempted to fit multiple spatial components to blended images, but this yielded component positions with poor accuracies (≥ 0.1 mas). Instead we found that using the the centroid position of the maser reference channel, which by definition is zero after phase referencing, improved the parallax fits compared to multi-component fits.

The reference channel emission for NGC 7538 (see Fig. 1) had a peak brightness of ≈ 6 Jy beam^{-1}, which was strong enough to produce good quality reference-phase solutions and yielded reasonable images of the background sources J2254+6209 and J2302+6405 (see Fig. 2). Formal fitting uncertainties for the positions of the background sources were $\sim$ 0.01 mas.

For NGC 7538, we first perfomed the parallax fit separately for the two background sources, J2254+6209 and J2302+6405. Next we produced a combined solution, which required fewer total parameters, since we constrained the solutions to have the same proper motion for the maser with respect to both background sources (as the background sources should have essentially zero proper motion). The error floors, which account for systematic errors in the relative postions, were 0.033 mas and 0.067 mas for the eastward and northward directions, respectively. Table 2 reports the results of these fits and Fig. 3 shows the data and the best fitting models. The errorbars for the positions in this figure include the error floors.

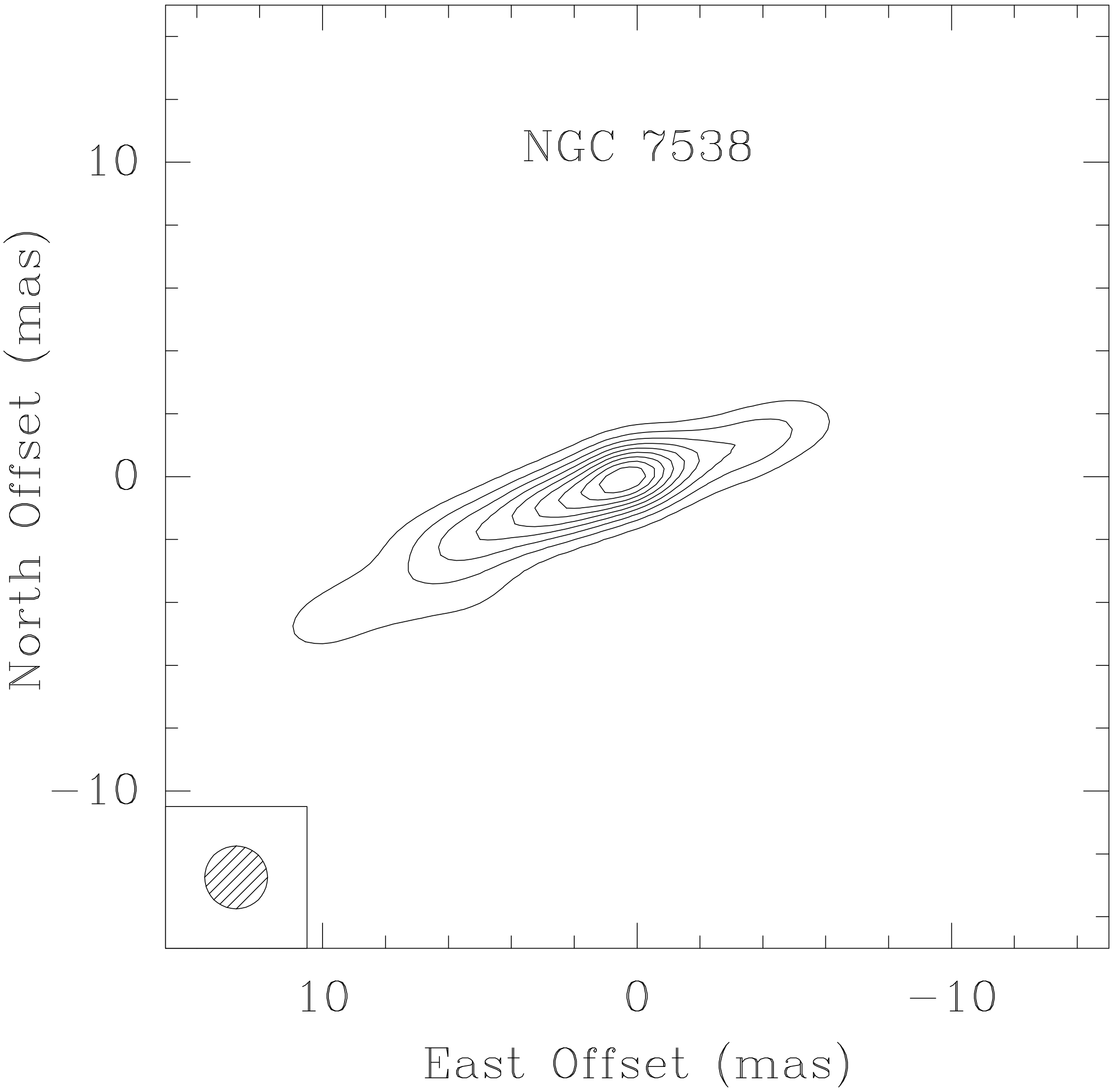

Fig. 1.— Self-calibrated image of the reference maser channel at $V_{\rm LSR} = -55.8$ km s^{-1} of NGC 7538 for the first epoch (2005 Sep. 9). Contour levels are at multiples of 10% of the peak brightness of 6.2 Jy beam^{-1}. The insert in the lower left shows the restoring beam.

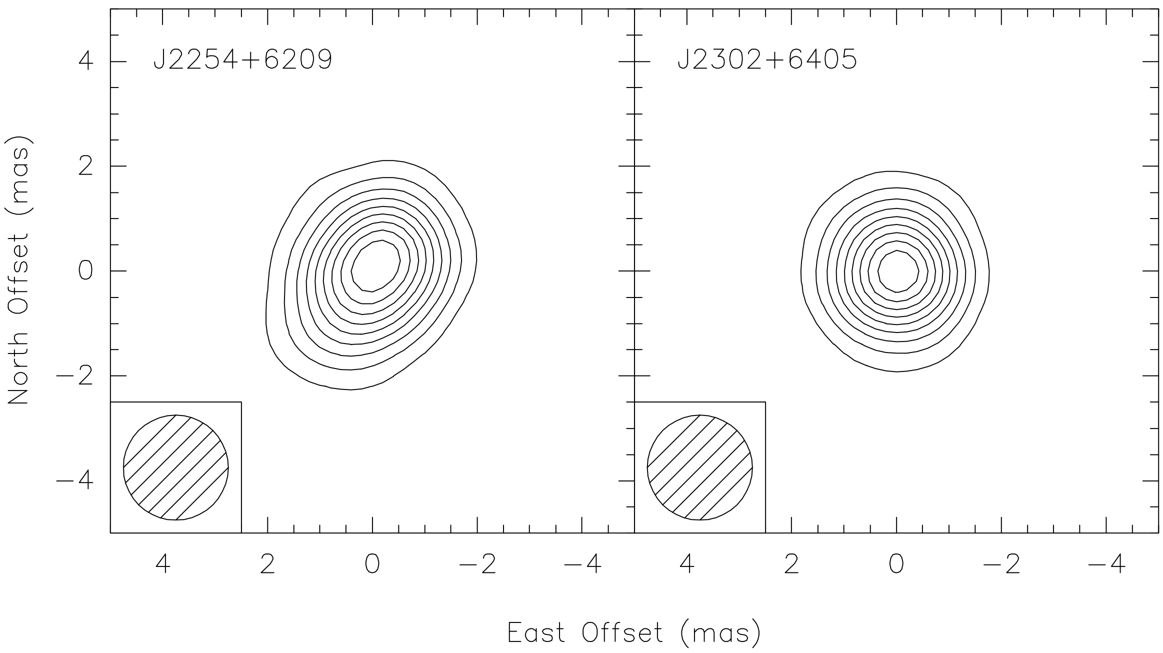

Fig. 2.— Images of the two background continuum sources phase referenced to the NGC 7538 maser. Source names are in the upper left corner and restoring beams are in the lower left corner of each panel. Both images are from the first epoch observations on 2005 Sep. 9. Contour levels of both images are at multiples of 10% of the peak brightness of 0.07 Jy beam^{-1} and 0.12 Jy beam^{-1} for the J2254+6209 and the J2302+6405 image, respectively.

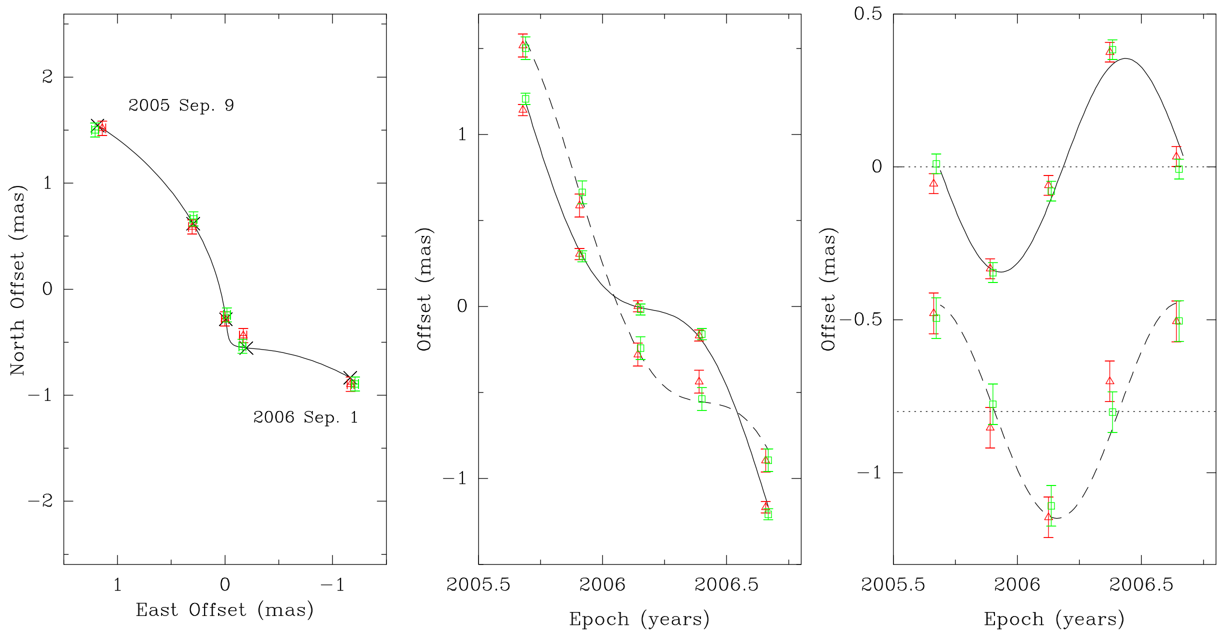

Fig. 3.— Results of the parallax fit for NGC 7538. For each plot, colored symbols indicate the position offset of the reference maser channel centroid; the errorbars have been scaled to give a reduced χ^2 of unity, as discussed in the text. *Red triangles* and *green squares* refer to measurements relative to the background quasars J2254+6209 and J2302+6405, respectively. **Left Panel:** Sky-projected motion of the maser. The *crosses* and the *continuous line* show the best-fit position offsets and the trajectory, respectively. The observing date of the first and last position are indicated. **Middle Panel:** The position offsets of the maser along the East and North direction versus time. The best-fit model of the variation of the East and North offsets with time is shown as *continuous* and *dashed* lines, respectively. **Right Panel:** Same as for the middle panel, but with the fitted slopes (proper motions) subtracted. The *dotted* lines indicate zero position offset. To avoid overlapping, the North offset data and model have been shifted to negative offsets.

3.2. Cep A

Since the brighest maser emission from Cep A was only ≈ 1 Jy beam^{-1} (see Fig. 4), the reference-phase solutions were marginal and this resulted in poor image quality for the two background sources (see Fig. 5), limiting the accuracy of position fits. Because the maser spots were fairly weak and possibly blended (see Table 5), we decided against image-plane fitting. As for NGC 7538, we simply used the centroid position of the maser reference channel for parallax fitting. Formal fitting uncertainties for the background continuum sources were ~ 0.05 mas for these images.

For Cep A, we perfomed the parallax fit separately for the two background quasars and also a combined solution. The error floors required to give fits with unity reduced χ^2 were 1.22 mas and 0.17 mas. The large eastward error floor for Cep A probably is caused by the large east-west extension of the maser and likely blending problems, and the Cep A parallax is effectively determined only by the north-south data. Table 3 reports results of these fits and Fig. 6 displays the data and the best fitting models. The errorbars for the positions in this figure include the error floors.

4. Discussion

4.1. Galactic Locations and Peculiar Motions

For both maser source, NGC 7538 and Cep A, our parallax distances are accurate to $\approx 5\%$. This is significantly better than the accuracy of photometric distances for these sources, which are typically accurate to 10–20% (Johnson 1957; Moreno & Chavarria-K. 1986).

The parallax distance of NGC 7538 of $2.65^{+0.12}_{-0.11}$ kpc is within the range of values reported in the literature: from 2.2 kpc (Moreno & Chavarria-K. 1986) to 2.8 kpc (Crampton et al. 1978). The kinematic distance of NGC 7538 is 5.6 kpc, assuming standard values for the rotation of the Galaxy ($R_0 = 8.5$ kpc and $\Theta_0 = 220$ km s^{-1}). At this distance, NGC 7538 would be well beyond the Perseus spiral arm, possibly in an "Outer" ("Cygnus") arm. However, the parallax distance is about a factor of two smaller than its kinematic distance, placing NGC 7538 in the Perseus spiral arm.

For Cep A, the methanol parallax distance of $0.70^{+0.04}_{-0.04}$ kpc is consistent with the most-cited value in the literature of 0.725 kpc (Johnson 1957). The distance to Cep A is also smaller than its kinematic distance of 1.1 kpc and places it in the "Local" (or "Orion") spur.

Table 2. NGC 7538 : Parallax & Proper Motion Fit

Maser V_{LSR} (km s^{-1})	Background Source	Parallax (mas)	μ_x (mas y^{-1})	μ_y (mas y^{-1})
−55.8	J2254+6209	0.371±0.026	−2.41±0.05	−2.41±0.12
−55.8	J2302+6405	0.414±0.019	−2.52±0.03	−2.47±0.13
−55.8	combined	0.378±0.017	−2.45±0.03	−2.44±0.06

Note. — Col. 1 reports the LSR velocity of the reference maser channel; Col. 2 indicates the background quasar whose data were used for the parallax fit: "combined" means that both quasars' data were used; Col. 3 reports the fitted parallax; Cols. 4 and 5 give the fitted proper motions along the East and North direction, respectively.

Table 3. Cep A : Parallax & Proper Motion Fit

Maser V_{LSR} (km s^{-1})	Background Source	Parallax (mas)	μ_x (mas y^{-1})	μ_y (mas y^{-1})
−4.2	J2254+6209	1.34±0.10	1.7±2.0	−3.8±0.2
−4.2	J2302+6405	1.51±0.11	−0.8±0.8	−3.6±0.2
−4.2	combined	1.43±0.08	0.5±1.1	−3.7±0.2

Note. — Col. 1 reports the LSR velocity of the reference maser channel; Col. 2 indicates the background quasar whose data were used for the parallax fit: "combined" means that both quasars' data were used; Col. 3 reports the fitted parallax; Cols. 4 and 5 give the fitted proper motions along the North and East direction, respectively.

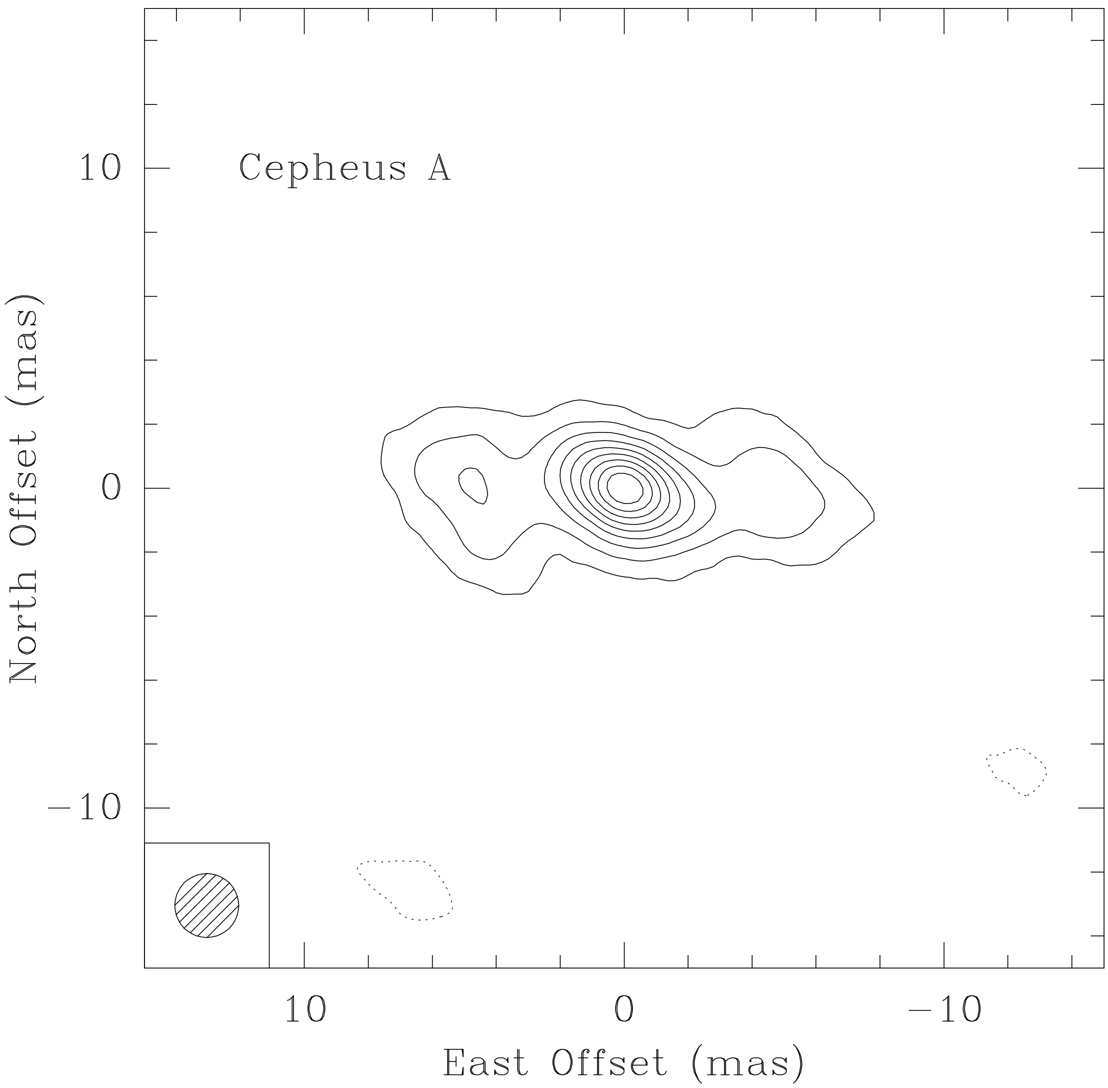

Fig. 4.— Image of the reference maser channel at $V_{\rm LSR} = -4.2$ km s^{-1} of Cep A for the first epoch (2005 Sep. 9). Contour levels are at multiples of 10% of the peak brightness of 0.9 Jy beam^{-1}. The insert in the lower left shows the restoring beam.

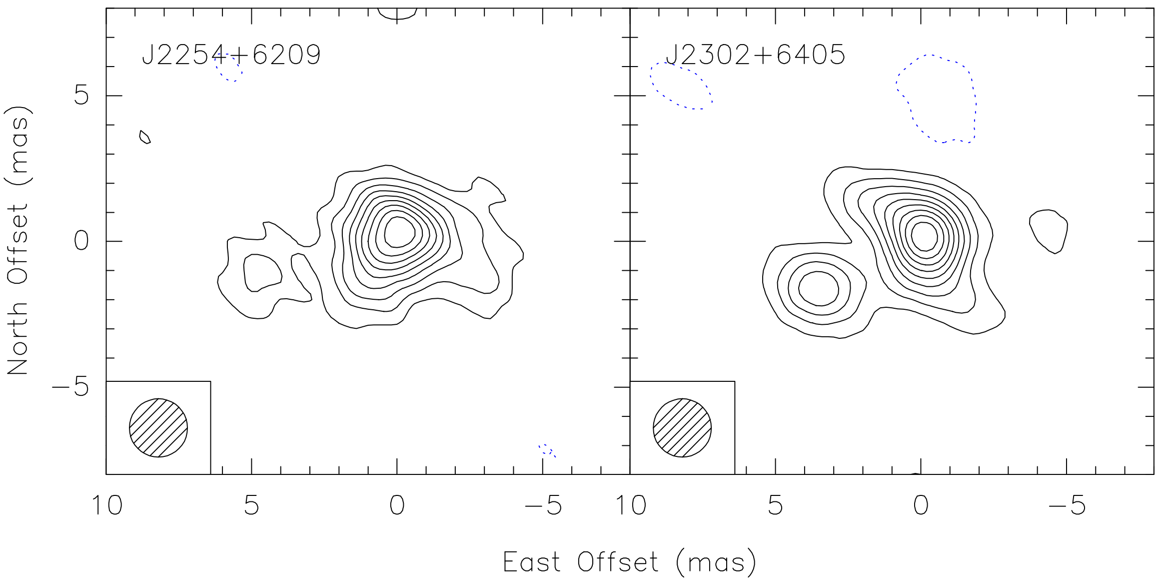

Fig. 5.— Images of the two background continuum sources phase referenced to the Cep A maser. Source names are in the upper left corner and restoring beams are in the lower left corner of each panel. Both images are from the first epoch observations on 2005 Sep. 9. Contour levels of both images are at multiples of 10% of the peak brightness of 0.03 Jy beam^{-1} and 0.04 Jy beam^{-1} for the J2254+6209 and the J2302+6405 image, respectively.

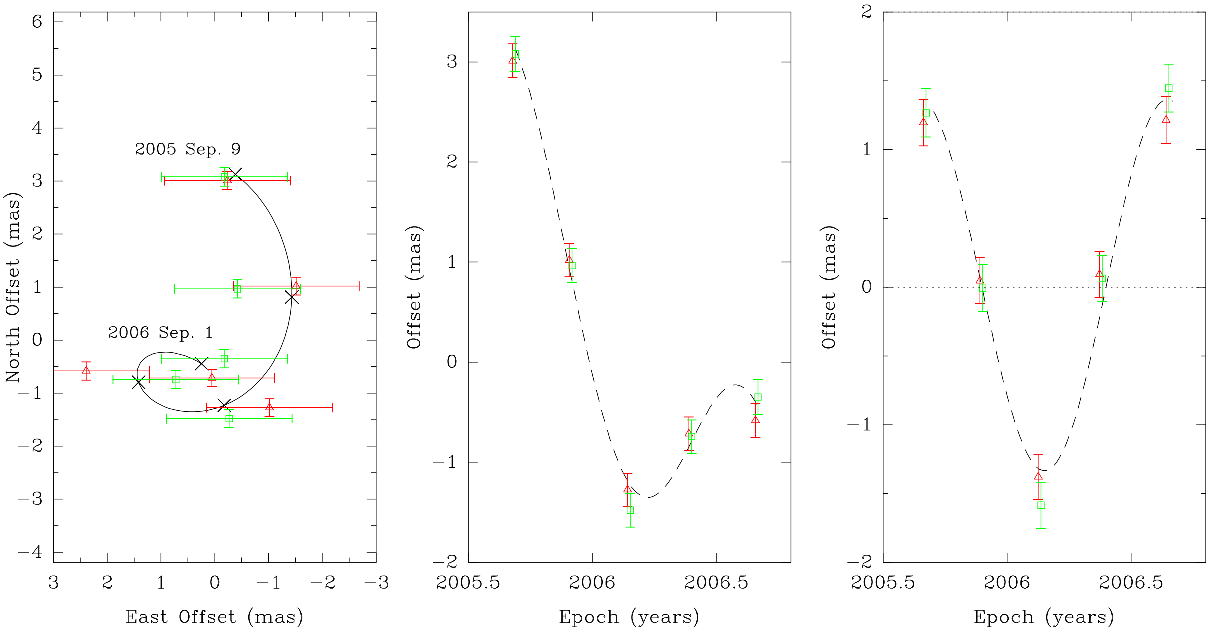

Fig. 6.— Results of the parallax fit for Cep A. For each plot, colored symbols indicate the position offset of the reference maser channel centroid; the errorbars have been scaled to give a reduced χ^2 of unity, as discussed in the text. *Red triangles* and *green squares* refer to measurements relative to the background continuum sources J2254+6209 and J2302+6405, respectively. **Left Panel:** Sky-projected motion of the maser. The *crosses* and the *continuous line* show the best-fit position offsets and the trajectory, respectively. The observing date of the first and last position are indicated. **Middle Panel:** The position offsets of the maser channel along the North direction are plotted versus time, with the *dashed* line showing the best-fit model. The eastward offsets had large (≥ 1 mas) uncertainties and are not shown. **Right Panel:** Same as for the middle panel, but with the fitted slope (proper motion) subtracted. The *dotted* line indicates zero position offset.

Combining the distances, LSR velocities and proper motions of the masers yields their locations in the Galaxy and their full space motions. Since internal motions of 12 GHz methanol masers are fairly small, typically ~ 3 km s^{-1}(Moscadelli et al. 2002), the maser motions should be close to that of their associated young stars. Given a model for the scale and rotation of the Milky Way, we can subtract the effects of Galactic rotation and the peculiar motion of the Sun from the space motions of the maser sources and estimate the peculiar motions of the maser star forming regions. We adopt the IAU values for the distance to the Galactic center ($R_0 = 8.5$ kpc) and the rotation speed of the Galaxy at this distance ($\Theta_0 = 220$ km s^{-1}) and the Hipparcos measurements of the Solar Motion (Dehnen & Binney 1998). For these parameters and a flat rotation curve, the peculiar velocity components for NGC 7538 are $(U_s, V_s, W_s) = (25 \pm 2, -30 \pm 3, -10 \pm 1)$ km s^{-1} and for Cep A are $(5 \pm 3, -12 \pm 3, -5 \pm 2)$ km s^{-1}, where U_s, V_s and W_s are velocity components toward the Galactic center, in the direction of Galactic rotation, and toward the North Galactic Pole, respectively, at the location of the source. The uncertainties for the peculiar motions reflect measurement errors for parallax, proper motion, and $V_{\rm LSR}$ (± 3 km s^{-1}assumed), but no systematic contribution from uncertainty in the Galactic model or Solar Motion.

NGC 7538 has large peculiar velocity components toward the Galctic center and counter to Galactic rotation. Cep A also has a significant peculiar motion counter to Galactic rotation. The implications of these peculiar velocities for models of Galactic rotation and structure will be discussed in a later paper, based on results for a large number of maser sources.

4.2. 12 GHz maser spatial distribution

Tables 4 and 5 give the strengths and velocities of maser spots detected in NGC 7538 and Cep A, respectively. The accuracy of the relative positions of maser spots within each source is usually limited by the complex spatial and velocity distribution of the maser emission and is typically 0.1 to 0.5 mas. At the distances of the masers and over our time baseline of 1 yr, this positional accuracy leads to an uncertainty in relative velocities of 2 to 7 km s^{-1} for NGC 7538 and 0.4 to 2 km s^{-1} for Cep A. As shown in Tables 4 and 5, internal motions are small (mostly < 5 km s^{-1}).

Table 4. Parameters of methanol 12 GHz maser spots detected in NGC 7538

Label	V_{LSR} (km s^{-1})	F_{int} (Jy)	$\Delta\alpha$ (mas)	$\Delta\delta$ (mas)	V_x (km s^{-1})	V_y (km s^{-1})
1	−55.8	18.8	0	0	0	0
2	−56.5	9.3	−5.9±0.4	1.7±0.1	−3±7	1±2
3	−55.8	3.8	4.7±0.4	−2.2±0.1	1±7	5±2
4	−55.8	2.7	8.2±0.4	-3.9±0.1	8±7	−4±2
5	−61.1	0.8	−92.1±0.4	−225.9±0.1		
6	−61.1	0.7	−72.0±0.4	−215.8±0.1	−3±7	1±3
7	−61.1	0.6	−88.3±0.4	−223.5±0.1		
8	−56.5	0.6	−35.3±0.4	11.5±0.2	3±8	0±3
9	−56.5	0.4	−38.9±0.5	9.0±0.2	1±8	0±3
10	−61.1	0.3	−75.2±0.4	−219.1±0.1	−1±7	6±3
11	−58.1	0.3	118.6±0.4	−178.9±0.2	0±8	4±3
12	−57.3	0.1	−71.8±0.4	20.1±0.2		
13	−58.1	0.1	124.7±0.5	−176.7±0.3		
14	−57.3	0.1	−77.0±0.4	21.6±0.2		
15	−58.1	0.1	121.4±0.5	−169.4±0.2		
16	−61.9	0.02	−282.3±0.4	124.0±0.2		

Note. — For each identified spot, Col. 1 reports the label number, increasing with decreasing spot intensity; Cols. 2 and 3 the LSR velocity and the integrated flux density; Cols. 4 and 5 the (eastward and northward) positional offsets evaluated with respect to the spot with label number 1; Cols. 6 and 7 the projected components along the East and North direction of the proper motion relative to the spot with label number 1. The derived absolute position of the maser reference spot (label number 1) is: R.A.(J2000) = $23^{h}\ 13^{m}\ 45\overset{s}{.}3622$, Dec.(J2000) = $61^{\circ}\ 28'\ 10\overset{''}{.}507$.

Table 5. Parameters of methanol 12 GHz maser spots detected in Cep A

Label	V_{LSR} (km s^{-1})	F_{int} (Jy)	$\Delta\alpha$ (mas)	$\Delta\delta$ (mas)	V_x (km s^{-1})	V_y (km s^{-1})
1	−4.2	1.8	0	0	0	0
2	−4.2	1.1	4.8±0.4	−0.1±0.2		
3	−1.9	1.1	−1348.3±0.5	150.4±0.3	−6±3	2±1
4	−4.2	0.9	−4.8±0.4	−0.2±0.2	−1±2	1±1
5	−4.2	0.5	−1168.0±0.5	−147.0±0.4		
6	−1.9	0.3	−1345.5±0.5	151.4±0.2		
7	−1.9	0.3	−1355.1±0.6	150.6±0.4		
8	−4.2	0.2	19.4±0.5	1.8±0.2		

Note. — For each identified spot, Col. 1 reports the label number, increasing with decreasing spot intensity; Cols. 2 and 3 the LSR velocity and the integrated flux density; Cols. 4 and 5 the (eastward and northward) positional offsets evaluated with respect to the spot with label number 1; Cols. 6 and 7 the projected components along the East and North direction of the proper motion relative to the spot with label number 1. The derived absolute position of the maser reference spot (label number 1) is: R.A.(J2000) = $22^{h}\ 56^{m}\ 18\overset{s}{.}0970$, Dec.(J2000) = $62^{\circ}\ 01'\ 49\overset{''}{.}399$.

4.2.1. Cep A

Fig. 7 shows the spatial distribution of the 12 GHz methanol masers detected toward Cep A overlaid on a map of the Cep A HW2 jet (Torrelles et al. 1996). The map of the Cep A HW2 jet was made by analyzing NRAO Archive VLA data from program AC534 observed in 1999. All spots concentrate in three clusters separated by $1\farcs35$ and $0\farcs15$ along the East and North direction, respectively. Two of the 12 GHz methanol maser spots appear to match in separation with those mapped by Minier et al. (2000) from VLBA observations in January 1999. However, one of Minier's spots does not appear in our map and, conversely, one of ours does not appear in his map. This indicates a time scale of order a decade for significant flux density variations. The detected maser clusters fall on both sides of the Cep A HW2 YSO, which is the most massive member of a group of protostellar objects inside a region of radius $\approx 1''$ (Comito et al. 2007). Given the complexity of this star-forming region, it is unclear whether the 12 GHz methanol masers are excited by a single or multiple protostellar objects.

4.2.2. NGC 7538

Fig. 8 shows the spatial distribution of the 12 GHz methanol masers detected toward NGC 7538 overlaid on a 15 GHz VLA A-configuration map of the ultra-compact HII region IRS 1 (Gaume et al. 1995). The continuum map was produced by analyzing NRAO Archive VLA data (program AF0413) from observations in 2004. The color code for the maser emission in Fig. 8 is centered (green) on the a systemic LSR velocity of -57.0 km s^{-1}, as indicated by high spectral resolution observations of the molecular emission from this core (Kameya & Takakubo 1988).

Toward NGC 7538 we detected 16 maser spots, of which 9 persisted throughout our observations. Comparing to previous methanol 6.7 and 12 GHz methanol observations of Minier et al. (2000, Fig. 1), we find his maser clusters A, B and C. We do not detect clusters D or E, which were previously identified only at 6.7 GHz. However, we do find a 12 GHz methanol maser spot at a (North, East) offset of $(-0\farcs23, 0\farcs13)$ that does not appear in Minier's map.

We confirm the possible velocity gradient seen in cluster A of Minier et al. (2000), indicating that this velocity/position structure is stable over a timespan of at least 7 years. This structure has been interpreted as either an edge-on rotating disk (Minier et al. 2000; Pestalozzi et al. 2004a,b) or a collimated outflow (De Buizer & Minier 2005). The expected proper motions for these two models would be quite different and they may offer a method

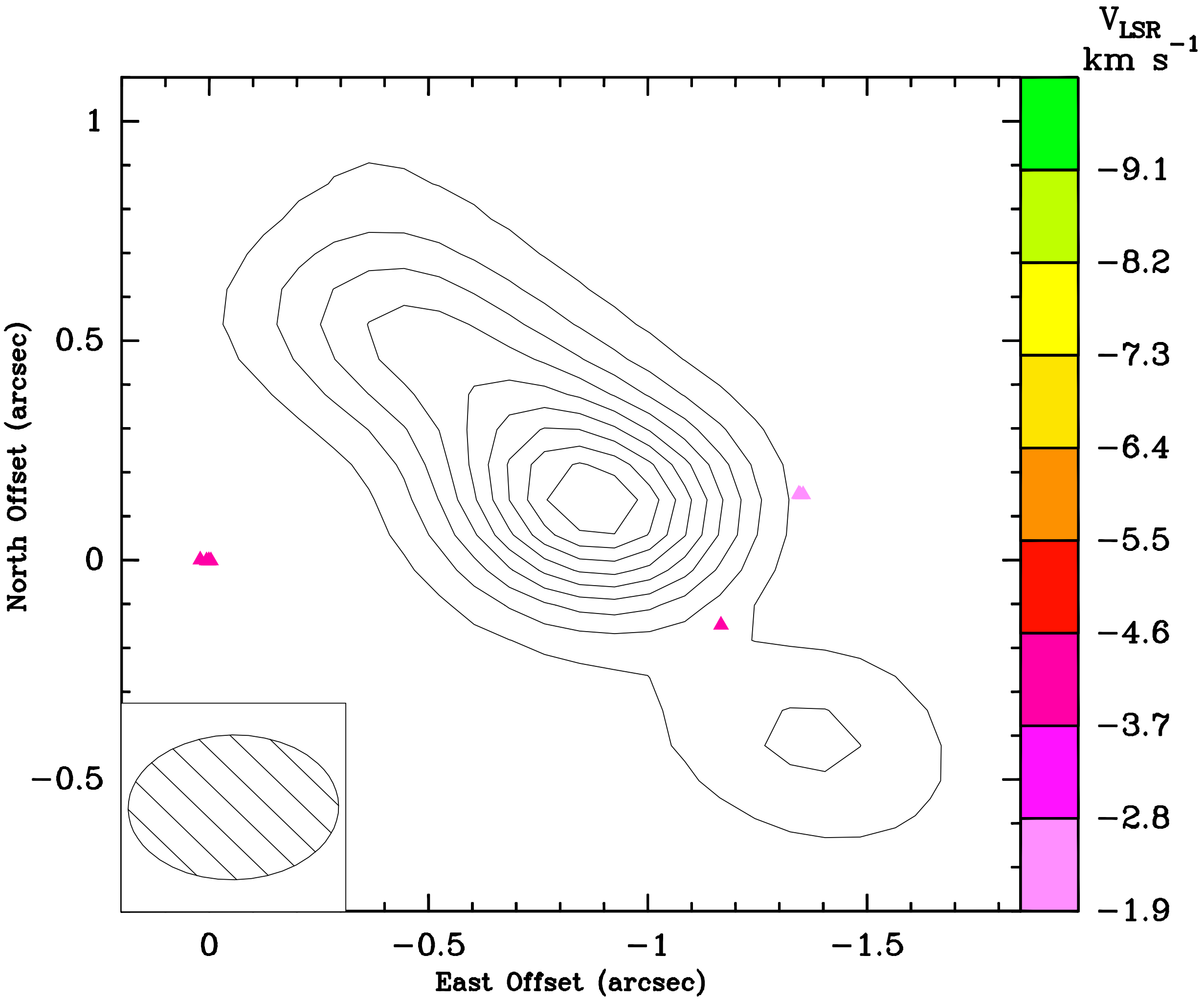

Fig. 7.— Cep A methanol 12 GHz maser distribution (*filled triangles*) plotted on an 8.4 GHz continuum VLA A-configuration image (*contours*) of the Cep A HW2 jet. Plotted levels of the continuum emission are at multiples of 10% of the peak brightness of 5 mJy beam^{-1}. Positions are relative to the most intense 12 GHz maser spot (label number 1 in Table 5). Different *colors* are used to indicate the maser LSR velocities, according to the color scale on the right-hand side of the plot. The color scale was chosen with the source rest velocity set to green and the maximum maser velocity set to purple. The insert at the bottom left corner shows the FWHM beam size of the VLA image. Maser spots in this source are weak and their velocity-averaged emission maps show little structure.

to discriminate between these models. However, since the spread in radial velocities across cluster A is only about 3 km s^{-1}, one would like proper motions with accuracies better than 1 km s^{-1}($<$ 0.1 mas y^{-1}). Future observations of the 12 GHz methanol masers with the VLBA should yield proper motions with such accuracies.

Andreas Brunthaler was supported by the DFG Priority Programme 1177.
Ye Xu was supported by Chinese NSF through grants NSF 10673024, NSF 10733030, NSF 10703010 and NSF 10621303.

REFERENCES

Comito, C., Schilke, P., Endesfelder, U., Jiménez-Serra, I., & Martín-Pintado, J. 2007, A&A, 469, 207

Crampton, D., Georgelin, Y. M., & Georgelin, Y. P. 1978, A&A, 66, 1

De Buizer, J. M. & Minier, V. 2005, ApJ, 628, L151

Dehnen, W. & Binney, J. J. 1998, MNRAS, 298, 387

Gaume, R. A., Goss, W. M., Dickel, H. R., Wilson, T. L., & Johnston, K. J. 1995, ApJ, 438, 776

Johnson, H. L. 1957, ApJ, 126, 121

Kameya, O. & Takakubo, K. 1988, PASJ, 40, 413

Migenes, V., Cohen, R. J., & Brebner, G. C. 1992, MNRAS, 254, 501

Minier, V., Booth, R. S., & Conway, J. E. 2000, A&A, 362, 1093

Moreno, M. A. & Chavarria-K., C. 1986, A&A, 161, 130

Moreno-Corral, M. A., Chavarria, K. C., de Lara, E., & Wagner, S. 1993, A&A, 273, 619

Moscadelli, L., Menten, K. M., Walmsley, C. M., & Reid, M. J. 2002, ApJ, 564, 813

Pestalozzi, M. R., Elitzur, M., Conway, J. E., & Booth, R. S. 2004a, ApJ, 603, L113

Pestalozzi, M. R., Elitzur, M., Conway, J. E., & Booth, R. S. 2004b, ApJ, 606, L173

Reid, M. J., Menten, K. M., Brunthaler, A., Zheng, X. W., Moscadelli, L., & Xu, Y. 2008, ApJ, accepted

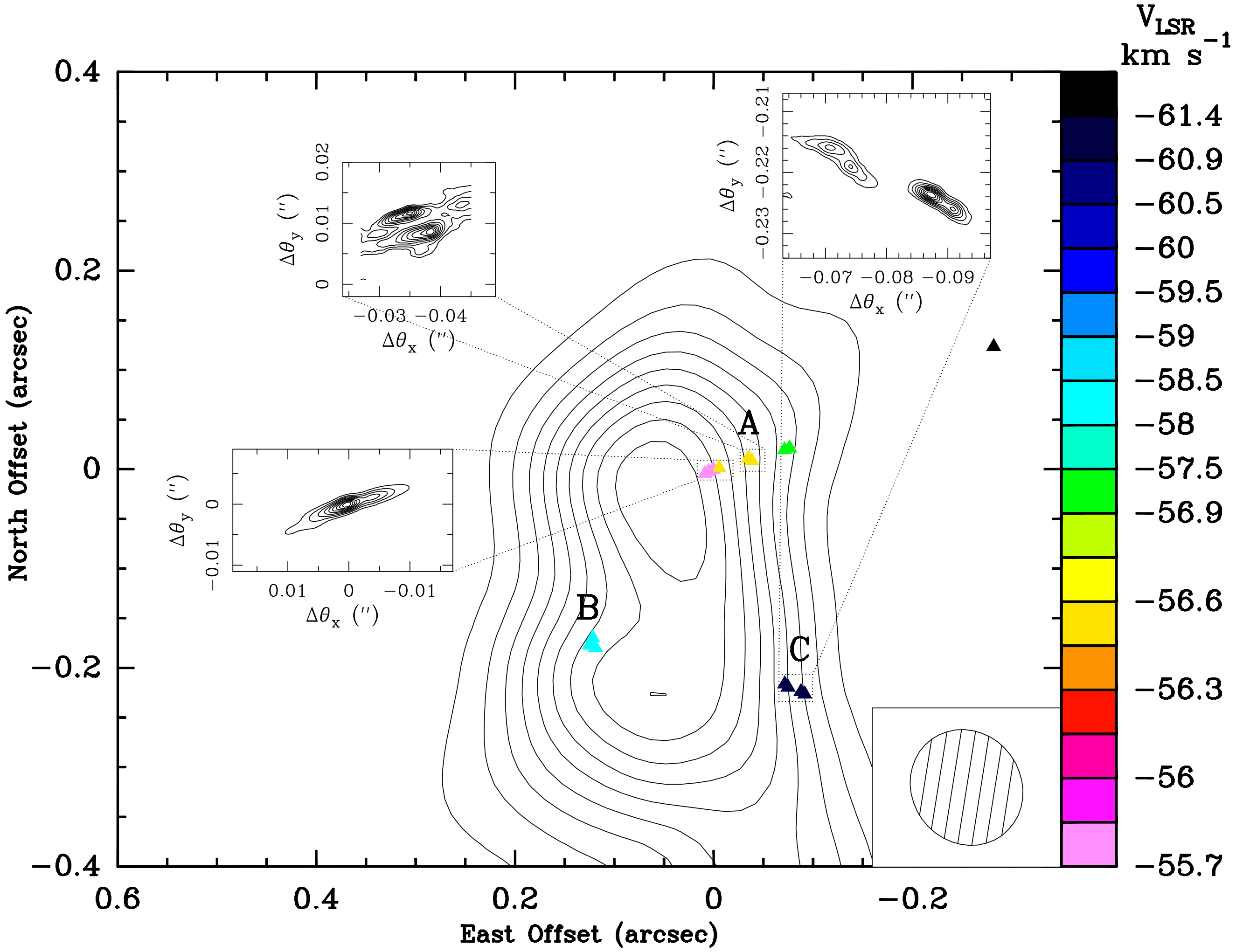

Fig. 8.— NGC 7538 12 GHz methanol maser distribution (*filled triangles*) plotted on a 15 GHz continuum VLA A-configuration image (*contours*) of NGC 7538 IRS1. Plotted levels of the continuum emission are at multiples of 10% of the peak brightness of 23 mJy beam^{-1}. Positions are relative to the most intense 12 GHz maser spot, labeled number 1 in Table 4. Different *colors* are used to indicate the maser LSR velocities, according to the color scale on the right-hand side of the plot. The 6.7 and 12 GHz maser clumps previously detected by Minier et al. (2000, Fig. 1) are labeled with capital letters A, B and C. The insert on the bottom right corner shows the FWHM beam size of the VLA image. **Small Panels:** The three small panels around the continuum image show the velocity-averaged emission of different groups of intense maser spots at the first observing epoch (2005 Sep. 9). Plotted levels are at multiples of 10% of the (velocity-averaged) spot peak intensity, corresponding to 1.6 Jy beam^{-1}, 0.13 Jy beam^{-1} and 0.2 Jy beam^{-1} for spots shown in the lower left, upper left and upper right panel, respectively.

Torrelles, J. M., Gomez, J. F., Rodriguez, L. F., et al. 1996, ApJ, 457, L107

Xu, Y., Reid, M. J., Zheng, X. W., & Menten, K. M. 2006, Science, 311, 54

Facilities: VLBA.